Influence of historic roof structures on the seismic behaviour of masonry structures

Alexandra I. Keller[1], Maria Adelaide Parisi[2], Eleftheria Tsakanika[3], Marius Mosoarca[1]

[1] Politehnica University Timişoara, Faculty of Architecture and Urban Planning, Timi□oara, Romania

[2] Politecnico di Milano, Department of Architecture, Built environment and Construction Engineering, Italy

[3] National Technical University of Athens, Department of Building Technology-Structural Design and Mechanical Equipment, Greece

Abstract

Historic buildings are complex structures where all the composing elements are working together. Studies made on heritage structures after seismic events show that timber roof structures strongly influence the seismic response of masonry structures, being able to reduce or enhance the out-of-plane displacement of the structure.

Starting from these observations, three different types of roof structures, from the 18th, 19th and 20th century, were introduced in the finite element simulation software SCIA Engineer. The roof structures were placed subsequently on the same an 18th-century masonry building with ground floor and two upper floors, respecting its geometric features. The simulations were performed considering successively rigid, hinged or sliding connections between the roof and the masonry structure. At the same time, the traditionally crafted joints of the roof structures were consecutively modelled as hinged, rigid and semi-rigid (determined using three different methods).

Ultimately the top horizontal displacement, inter-story drift and damage level of the masonry structure were compared. The main scope of the study was to observe if roof structures would have an influence on the seismic behaviour of the masonry building and if the compared parameters would suffer any changes depending on the used roof structure type, roof to wall connection and joints axial stiffness.

Keywords

Seismic engineering, Timber structures, Brickwork & masonry

Introduction

In historic buildings, all the composing structural elements are interlinked and are influencing each other and the global structural behaviour of the building. Despite this, heritage buildings are assessed individually ignoring the roof structure, while roof structure assessment methodologies are also treating them as independent systems with only a little attention paid to the link between the building and the roof (Cruz *et al.* 2015; D'Ayala and Riggio 2015; Riggio *et al.* 2018).

Still in recent years studies performed after seismic events showed that roof structures can enhance the effects of the seismic loads triggering the out of plane failure of exterior walls (Parisi *et al.* 2008; Parisi *et al.* 2012; Parisi and Chesi 2014; Giresini *et al.* 2016; Parisi *et al.* 2016). On the other hand, studies also show that the use of timber elements connected to masonry walls can reduce the effect of the seismic loads (Touliatos 1993; Touliatos 2005; Tonna and Chesi 2015).

Therefore, starting from three characteristic roof structures from Timisoara, placed on an 18th-century masonry structure, the study aims to identify how roof structures in this area are influencing the seismic behaviour of unreinforced masonry structures.

1. Case study

For the study, a historic building from the city centre of Timisoara was considered, on top of which three roof structures from different periods were placed in order to be able to make a comparison of the effects of roof structures from various construction periods on the seismic behaviour of the masonry structure.

1.1. The evaluated building

The analysed structure was built in the 18th century, comprising all the specific elements of that period. Therefore, it has an L shape, with the main wing facing the street and a secondary annexe building facing the interior courtyard. The main building has an underground level and three levels above ground while the annexe building has only two floors above ground.

The structure of this building was made using brick masonry with walls having a width of 90 centimetres on the ground floor decreasing down to 45 centimetres on the second floor. The floors of the building also change with the height of the building: for the underground and the ground storey a cross-vaulted floor was used and the two upper levels present a timber beam flooring (Gaivoronschi *et al.* 2013). In order not to take the torsional effect due to the interaction between the two wings into consideration, the analysis was only performed on the main wing of the building.

1.2. The used roof structures

The three roof structures were chosen to be as different as possible in order to better understand the influence of various roof types on the seismic behaviour of the chosen masonry building.

The first roof (Figure 1) was typically built at the end of the 18th century. The structure is composed of 2 layers of timber elements, the outer comprising only rafters connected by a collar beam, forming the support for the roof envelope and the inner layer, which is composed of compound rafters and straining beam, enhancing the rigidity of the frame (Figure 1a). Secondary frames, placed between the main ones, preserve the outer layer elements (Figure 1b). All frames, are connected in the inferior part by a tie beam and in the longitudinal direction by additional eaves and intermediate purlins (Andreescu *et al.* 2016).

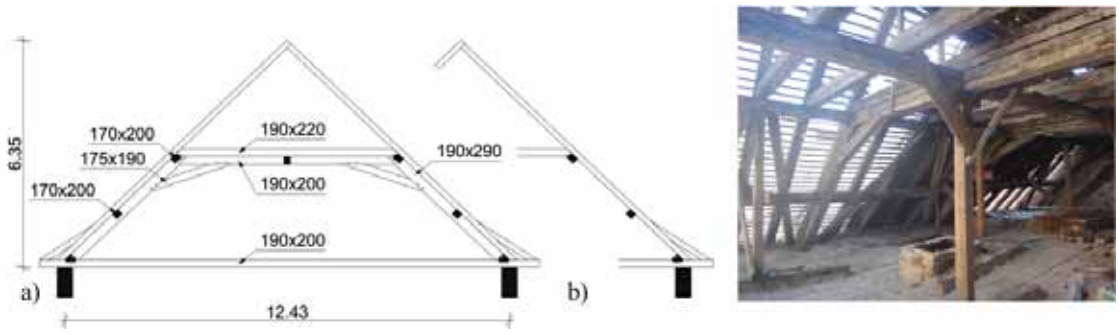

Figure 1 First roof structure (a) main; b) secondary frame)

The second roof structure (Figure 2) was built in the 19th century, presenting an evident change of the structural type. A clear difference between main (Figure 2a) and secondary frames

(Figure 2b) is also in this case visible, the main ones being composed of rafters supported by struts which are additionally connected to the tie beam by compound rafters. An additional collar beam is also inserted in the upper part of the frame. The secondary frames, on the other hand, are only composed of rafters, connected to the main ones by eaves, intermediate and ridge purlins.

The peculiar feature of this roof structure is the use of a grid of timber elements on the top of the exterior walls of the building, which is additionally increasing the rigidity of the top part of the walls.

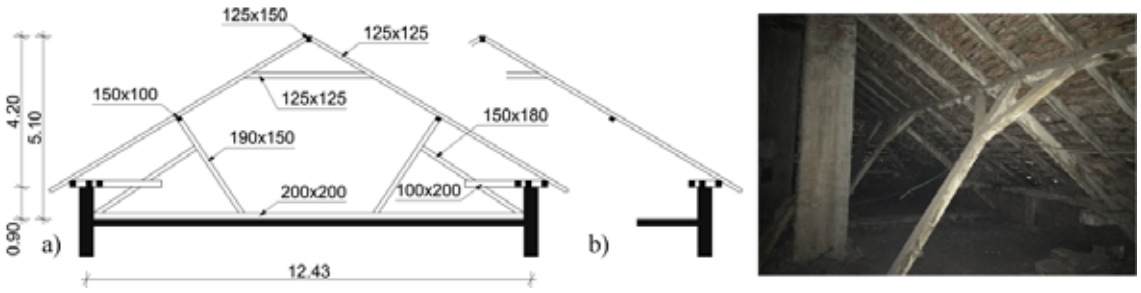

Figure 2 Second roof structure (a) main; b) secondary frame)

The third roof structure (Figure 3) belongs to a building which changed its appearance at the beginning of the 20th century. The roof structure presents a clear example of a queen post purlin roof, composed of rafters, compound rafters and two posts connected in the upper part by a collar beam and in the inferior part by a tie beam. Due to the significant height of the roof, an additional king post was placed in the upper part (Figure 3a). The secondary frames (Figure 3b) are only composed of rafters connected by purlins (Keller and Mosoarca 2017).

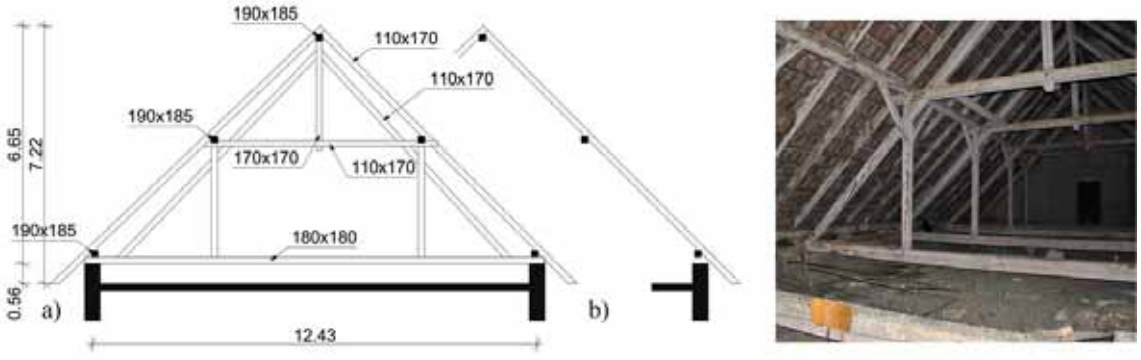

Figure 3 Third roof structure (a) main; b) secondary frame)

2. Finite element simulations

Four three-dimensional models of the masonry structure were made using the finite element analysis software SCIA engineer (Nemetschek 2013) in order to be able to compare the seismic response of the building without roof structure and subsequently with each of the three chosen roofs, by using a seismic spectral analysis with lateral forces. The models were made respecting the geometrical properties of the main wing of the masonry building and the cross-section of the timber elements (Figure 4).

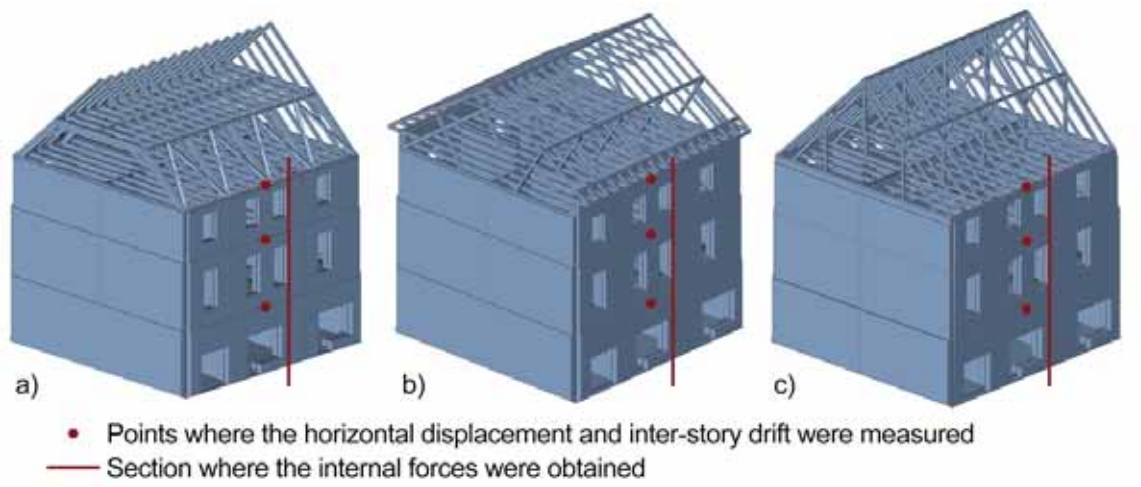

Figure 4 The models of the finite element simulations (a) first; b) second; c) third roof structure)

Due to the reduced number of experimental tests concerning the mechanical properties of timber elements in Timisoara and due to the diverse periods in which the roof structures were built, for the study the minimum strength class according to EN 338 (Comite Europeen de Normalisation 2016), D18 was chosen and for the masonry, historic brickwork with lime mortar was considered (Table 1).

Table 1 Mechanical properties of the used materials

Oak		
Self-weight		5.7 kN/m³
Tensile-strength	$f_{t,0,k}$	11.00 N/mm²
Compressive-strength	$f_{c,0,k}$	18.00 N/mm²
	$f_{c,90,k}$	4.80 N/mm²
Bending-strength	$f_{m,k}$	18.00 N/mm²
Shear-strength	$f_{v,k}$	3.50 N/mm²
Modulus of elasticity	$E_{0.05}$	9500 N/mm²
Mean modulus of elasticity	$E_{0,mean}$	8 000 N/mm²
	$E_{90,mean}$	630 N/mm²

Masonry		
Self-weight		1800 kg/m³
Modulus of elasticity	$E_{0.05}$	750 N/mm²
Compressive-strength	$f_{c,0,k}$	1583 kN/mm²
Partial safety factor	γ_M	1.00
Shear-strength	$f_{v,k}$	200 kN/mm²
Flexular-strength	$f_{x,k1}$	180 kN/mm²
	$f_{x,k1}$	360 kN/mm²
Shear-modulus	G_{mean}	300 N/mm²

Shear-modulus	G_{mean}	590 N/mm²
Self-weight		5.7 kN/m³

2.1. Loads

For the study the seismicity of the Banat region was considered, the second seismic area of Romania (Narita *et al.* 2016; Apostol *et al.* 2019a; Mosoarca *et al.* 2019). Here, mainly shallow, crustal type earthquakes are happening, with a peak ground acceleration of 0.2g (Apostol *et al.* 2019b).

The seismic response spectrum used for the performed simulations was determined according to the Romanian Seismic Design Code (2013) (Figure 5). Due to the layout of the assessed building and its irregular shape, the behaviour factor was considered 1.65.

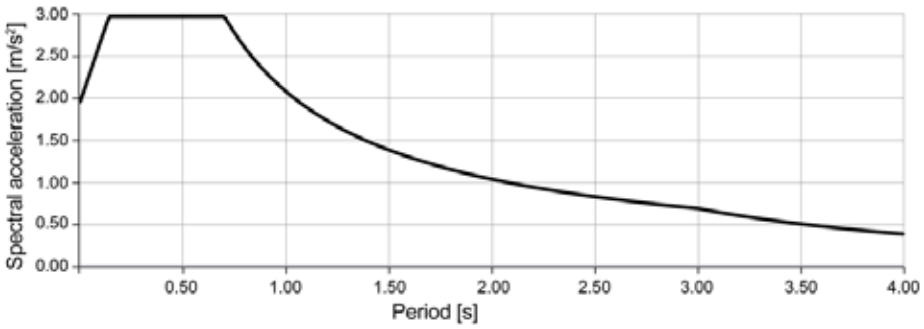

Figure 5 Seismic response spectrum for Timisoara

The linear static analysis was performed using a load combination which considered the self-weight, automatically determined by the software according to the density of the material, dead loads, live loads and snow loads, determined according to the national codes. The combination was determined using the following equation also considering the correction coefficients of the applied loads:

2.2. Semi-rigid modelling of timber joints

In order to better understand the structural behaviour of the historic roof structures, three different support typologies were considered for the performed numerical simulations: rigid, sliding (Wallner *et al.* 2014) and hinged and sliding. Subsequently for all the support scenarios,

145 the traditionally crafted timber joints were considered rigid, hinged and semi-rigid determined
146 using 3 different equations, according to Hölzer (Holzer 2015; Holzer 2016), the component
147 method (Descamps and Lemlyn 2009; Branco and Descamps 2015) and the equations
148 developed by Heimeshoff and Köhler (Heimeshoff and Kohler 1989; Meisel 2015).
149 In order to be able to identify the assessed scenarios, each one of them was associated with
150 two numbers, the first one representing the support typology and the second number the joint
151 type (Table 2).
152
153 **Table 2** Names of the assessed scenarios

SCENARIOS	1. Rigid-support	2. Sliding-support	3. Hinged-sliding-support
1. Rigid-joints	S1.1.	S1.2.	S1.3.
2. Hinged-joints	S2.1.	S2.2.	S2.3.
SEMI-RIGID JOINTS			
3. Hölzer	S3.1.	S3.2.	S3.3.
4. Component-method	S4.1.	S4.2.	S4.3.
5. Heimeshoff&Kohler	S5.1.	S5.2.	S5.3.

154
155 Hölzer (Holzer 2016) considers that it is not possible to accurately determine the stiffness of
156 individual joints and the effort is not necessary. He therefore proposes stiffness values for each
157 type of joint which would be useful in determining the general structural behaviour of historic
158 timber roof structures (Table 3).
159
160 **Table 3** Axial stiffness of timber joints Hölzer [kN/m]

Joint type	Tensile	Compression	
		90°	30°
Notch joint	0	45	
Tenon-Mortice joint	5/peg	60	20
Lap joint	5/peg	60	20

161
162 According to the component method, the axial stiffness of timber joints can be determined
163 based on the mechanical properties of the used timber and the geometric properties of the joints
164 (contact surface and connection angle) (Branco and Descamps 2015).
165 It can be determined using the following equation:

$$k_{ax} = \frac{E_{\alpha} \times}{l}$$

Where Eα represents the elastic modulus of the timber at an α angle with the fibre; S, the compressed surface of the joint, determined according to the joint type and l the notch length, where the deformation caused by compression is assumed to occur:

$$E\alpha = \frac{E_0}{\cos^2 \alpha + \frac{E_0}{E_{90}} \sin^2 \alpha}$$

$$S = \frac{A_{rafter}}{\sin \alpha}$$

$$l = \frac{h}{2 \sin \alpha}$$

In the case of tenon and mortise joints, the vertical load is transferred through the upper contact surface (A_{vert}) loaded at an α angle to the grain. A gap between tenon and mortise can be assumed according to Branco and Descamps (Branco and Descamps 2015), so only the upper contact surface was considered. On the other hand, the horizontal load is transferred through the head of the tenon (A_{horiz}).

$$k_{horiz} = \frac{E_\alpha \times A_{horiz}}{l_{horiz}}$$

Where $l_{horiz} = H/2$

$$k_{vert} = \frac{E_\alpha \times A_{vert}}{l_{vert}}$$

Where $l_{vert} = h/2$

Heimeshoff and Köhler (Heimeshoff and Kohler 1989) conducted in 1989 an extensive experimental campaign in order to identify the behaviour of historic timber joints. An equation was subsequently developed, which could be used to determine the axial stiffness of a historic timber joint, considering only its geometric properties:

$$k_{ax} = (45.2 - 42.1 \times sin^2 \alpha) \times \frac{b}{12} \times (1 + \frac{t_v - 2.34}{2.34} \times 0.1)$$

Where k_{ax} is the axial stiffness of the joint, in kN/mm; α is the angle between the elements of the joint, b the width of the base element in cm and t_v the depth of the notch in cm.

Subsequently, after studies performed at the Graz University of Technology (Wallner *et al.* 2014), the equation was adapted for tenon and mortise joints, considering the width of the compressed surface and the compressed area of the tenon

$$b = b_{inserted\ element} - b_{tenon}$$

$$t_v = \frac{A^*}{b_{inserted\ element}}$$

185 Where

$$A^* = b_{inserted\ element} \times t + b_{tenon} \times t_{tenon}$$

186 After the axial stiffness was determined using the three different methods, the high differences
187 between the results were observed. (Table 4). Even though both the component method and
188 the equations developed by Heimeshoff and Köhler take the geometric properties of the timber
189 joint into consideration, the main difference and reason of the high discrepancy of the result is
190 that the component method is also taking the mechanical properties of the timber into
191 consideration.

192 **Table 4** Axial stiffness of timber joints of the three roof structures [kN/m]

	Component method	Heimeshoff and Köhler	Hölzer
Roof structure 1			
rafter-tie beam	316,658	50,421	60,000
compound rafter - tie beam	658,904	56,442	60,000
counterbrace - compound rafter	997,826	34,111	20,000
counterbrace - straining beam	3,098,916	37,278	20,000
straining beam - compound rafter	317,311	26,360	60,000
collar beam - rafter	289,113	25,113	60,000
rafter- rafter	141,931	3,039	60,000
Roof structure 2			
compound rafter - tie beam	575,914	50,925	20,000
brace - compound rafter	388,812	27,036	20,000
compound rafter - strut	123,408	3,162	60,000
rafter - wall plate	461,168	22,925	20,000
post - rafter	86,029	2,145	60,000
collar beam - rafter	662,028	22,808	20,000
rafter- purlin	130,916	9,390	60,000
strut - tie beam	186,850	15,067	60,000
Roof structure 3			
passing brace - tie beam	214,714	43,385	20,000
passing brace - post	265,950	43,385	20,000
passing brace - collar beam	209,065	2,875	60,000
passing brace - king post	228,001	2,875	60,000
rafter - tie beam	236,759	17,235	20,000
rafter - collar beam	228,001	14,762	20,000
rafter - king post	227,129	4,949	60,000
king post - collar beam	137,876	2,918	60,000
post - tie beam	116,281	2,675	60,000

193

3. Influence on the seismic behaviour of the assessed building

Subsequently, five main parameters were assessed: the horizontal displacement and inter-storey drifts of every floor, the deformed shape of the building and the damage level and internal forces recorded on the masonry walls. They were assessed for the building with no roof, the building with the three roof structures with a full cross section and the 20% decayed roofs, according to the observations of Branco et al. (Branco *et al.* 2010).

3.1. Displacement

In the first part of the study, the horizontal displacement of every floor of the masonry building was evaluated. (Table 5).

For the first roof structure, the displacement of the first floor is quite similar for all the assessed scenarios varying of about 5% between the complete section roof structure and the reduced section one (Figure 6). At the second floor, the complete cross-section scenarios present a mean reduction of the horizontal displacement of 10%, while the scenarios with decayed timber elements is presenting a reduction of the horizontal displacement of only 5%. The increase of the displacement, in this case, is around 10 up to 30%, compared with the complete cross-section roof. Subsequently, the third floor presents the clearest decrease of the top horizontal displacement of the building, around 50% for the complete cross-section timber elements and around 40% in the reduced cross-section case. The decay of the timber elements is, therefore, increasing the top horizontal displacement up to 30%, compared to the full cross-section.

The horizontal displacement analysis of the masonry building with the second roof structure showed a different type of behaviour compared to the first one. The complete cross-section of the timber elements causes a 5% increase of the horizontal displacement at the 1st floor while the reduction of the cross section is increasing this displacement to up to 10%. Only above the 2nd floor the influence of the roof structure can be identified in this case, the roof structure with complete cross-section reducing the horizontal displacement at the 2nd floor with 5% and at the 3rd floor with up to 40%. The decayed roof structure (Figure 6), on the other hand, is still

223 increasing the horizontal displacement with 20% at the 2nd floor and is only reducing it on the
224 3rd floor with also 40%. The differences between the 2 cases range between 10 and 20%, the
225 main difference between them being on the 3rd floor, where the decayed structure is reducing
226 the horizontal displacement with up to 5% compared with the horizontal displacement obtained
227 with the complete cross-section roof.
228 The building with the 3rd roof structure is presenting a similar behaviour to the no roof structure
229 case, the horizontal displacement raising continuously until the top of the structure. The
230 complete cross-section roof is presenting a 10% reduction of the horizontal displacement at the
231 1st floor, 15% reduction at the 2nd and 30% and the 3rd floor. The decayed roof, on the other
232 hand, is presenting no changes at the 1st floor, a slight increase of 5% at the 2nd floor and
233 ultimately but 25% decrease of the horizontal displacement at the 3rd floor (Figure 6). By
234 comparing the two states of conservation of the roof structure, it was observed that the
235 displacement of the building with the decayed roof is with 15% higher at the 1st floor, 30%
236 higher at the 2nd floor but is decreasing with between 5 and 20% at the 3rd.
237
238 **Table 5** Displacement analysis and comparison

	No roof	Roof 1 Displacement [mm]		Roof 2 Displacement [mm]		Roof 3 Displacement [mm]	
		100%	-20%	100%	-20%	100%	-20%
1st floor	2.18	≈2.08	≈2.15	≈2.29	≈2.42	≈1.98	≈2.20
Compared to 100%			>+5…20%		>+10%		>+5…15%
Compared to no roof		-5%	No difference	+5%	+10%	-10%	No difference
2nd floor	7.28	≈6.55	≈7.05	≈7.77	≈8.69	≈6.31	≈7.62
Compared to 100%			>+10…30%		>+10…20%		>+20…30%
Compared to no roof		-10%	-5%	-5%	+20%	-15%	+5%
3rd floor	19.86	≈10.22	≈11.81	≈11.44	≈11.33	≈15.43	≈14.44
Compared to 100%			>+5…30%		<-5%		<-5…20%
Compared to no roof		-50%	-40%	-40%	-40%	-20%	-25%

239

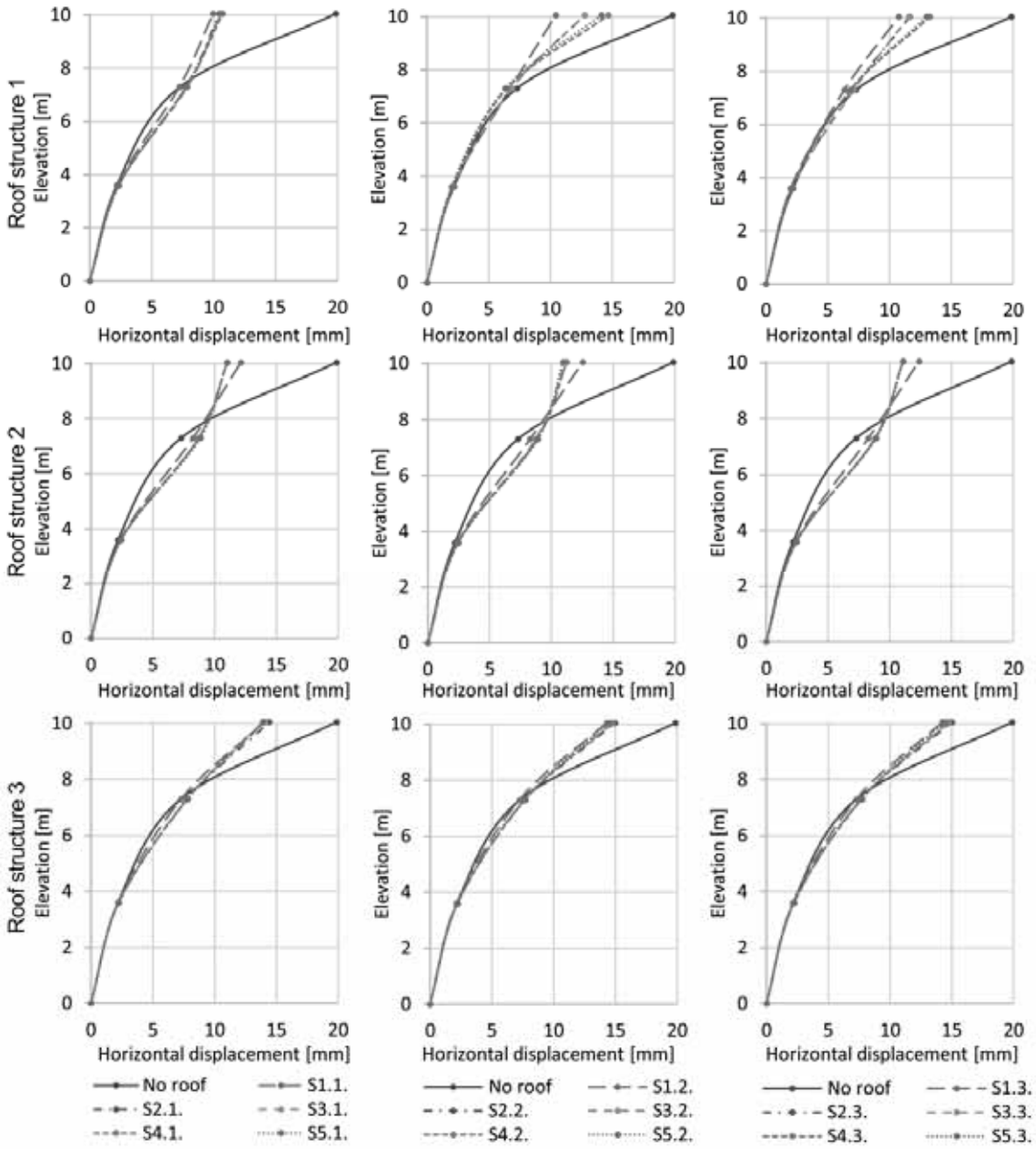

240

241 **Figure 6** Displacement of the masonry building considering all three decayed roof structures

242

243 ***3.2. Inter-story drift***

244 Starting from the displacement, the inter-story drift of every floor was determined.

245 Compared to the building without a roof, the presence of the first roof structure is causing a

246 different type of behaviour, the inter-story drift decreasing 5% at the 1st floor, 10% at the 2nd

247 and 70% at the 3rd floor. A slight difference between the two states of conservation of the roof

248 structure was also observed mainly and the 2nd and 3rd floor where the inter-story drift is

increasing with up to 40%. Still, even the decay of structure is causing a reduction of the inter-story drift at the 3rd floor with up to 60% compared to the no roof structure case.

The presence of the second roof structure is causing a similar behaviour like the first one with inter-story drift raising continuously until the 3rd floor, being up to 5% lower at the 1st floor, 10% at the 2nd and ultimately 70% at the 3rd floor. In this case, the decay of the timber element is raising the inter-story drift at the 1st and 2nd floor with up to 20% but is decreasing the drift with 80% on the 3rd floor. The decayed structure proves to have improved the behaviour of the masonry building on the 3rd floor, presenting a drift up to 30% lower compared to the ideal roof.

The third roof structure proves out to have the lowest influence on the inter-story drift of the building, reducing it with up to 10% at the 1st floor, 15% of the 2nd and only 25% at the 3rd floor. The decayed roof, on the other hand, is also proving to have limited influence on the 1st and 2nd floor, increasing the inter-story drift with 10% of the 1st floor and 30% at the 2nd but significantly decreasing it at the 3rd floor with 45%. This decay of this roof structure is proving to also significantly reduce inter-story drift of the 3rd floor, with up to 40% compared to the complete cross-section timber element roof, but the 1st and 2nd floor are more affected due to the increased inter-story drift.

Table 6 Inter-story drift analysis and comparison

	No roof	Roof 1 Inter-story drift [mm]		Roof 2 Inter-story drift [mm]		Roof 3 Inter-story drift [mm]	
		100%	-20%	100%	-20%	100%	-20%
1st floor	2.18	≈2.08	≈2.15	≈2.29	≈2.42	≈1.95	≈2.20
Compared to 100%			> +5%		>+5%		>+5…10%
Compared to no roof		-5%	No difference	-5%	+10%	-10%	No difference
2nd floor	5.10	≈4.47	≈4.90	≈5.48	≈6.27	≈4.37	≈5.42
Compared to 100%			>10…+40%		>+10…+20%		>+25…30%
Compared to no roof		-10%	-5%	-10%	+20%	-15%	+5%
3rd floor	12.58	≈3.67	≈4.75	≈3.67	≈2.64	≈9.39	≈6.82
Compared to 100%			>+15…+20%		<-20…-30%		<-20…40%
Compared to no roof		-70%	-60%	-70%	-80%	-25%	-45%

3.3. Deformed shape

While analysing the deformed shape of the building, it was observed that each roof structure is influencing the deformation of the masonry building in a different way and that the state of conservation of the timber elements is also having a significant influence on the deformation

(Table 7). The building with no roof is presenting flexural deformation, with inter-story drifts continuously raising until the top of the masonry structure.

The presence of the first roof structure is causing a shear deformation for most of the assessed scenarios, but there are still cases where the masonry structure is presenting flexural deformation. The decay of the timber elements, on the other hand, is not influencing the deformation of the building, except for the S2.2 and S3.2 scenarios (see Table 2), where the deformation is changing to flexural.

The second roof structure has a more evident influence on the deformation of the masonry structure causing a shear deformation for almost all scenarios, except S1.2 and S1.3, where the structure is suffering a flexural deformation. In this case, for the decayed timber elements, the deformation also changes for these two scenarios to shear.

The third roof structure, with full and reduced cross-section, is presenting the most similar deformation to the no roof structure case, all the assessed scenarios presenting flexural deformation of the building.

Table 7 Deformed shape of the masonry building

	Roof 1		Roof 2		Roof 3	
	100%	-20%	100%	-20%	100%	-20%
S1.1.	Shear	Shear	Shear	Shear	Flexural	Flexural
S2.1.						
S3.1.						
S4.1.						
S5.1.						
S1.2.	Shear	Shear	Flexural	Shear	Flexural	Flexural
S2.2.	Shear	Flexural	Shear			
S3.2.	Shear	Flexural	Shear			
S4.2.	Flexural	Flexural	Shear			
S5.2.	Flexural	Flexural	Shear			
S1.3.	Flexural	Flexural	Flexural	Shear	Flexural	Flexural
S2.3.	Shear	Shear	Shear			
S3.3.	Shear	Shear	Shear			
S4.3.	Flexural	Flexural	Shear			
S5.3.	Flexural	Flexural	Shear			

3.4. Damage level

Considering the ranges of the inter-story drift limit states presented by Vicente et al. (Vicente *et al.* 2014), according to the Eurocode 8, Part 3 and the FaMIVE procedure and based on

292 experimental tests performed on masonry structures, the damage level of the assessed
293 structure was determined without and with the 3 chosen roof structures.
294 First, the damage level of the building without a roof structure was assessed. Considering the
295 in-plane prevalent behaviour of the structure, it was observed that it would suffer significant
296 damage at the 3rd floor for all the limit states, while the FaMIVE limit state is also presenting
297 significant damage at the 2nd floor. Out-of-plane, this structure would only suffer significant
298 damage according to the experimental limit state on the 3rd floor while the combined prevalent
299 behaviour also shows the presence of significant damage on the 3rd floor.
300 The presence of the 1st roof structure is significantly improving the damage state of the
301 masonry structure. Therefore, it was observed that in-plane the building would suffer significant
302 damage mainly at the 3rd floor only according to the FaMIVE limit state, while the out of plane
303 prevalent behaviour is presenting no damage at all. The combined prevalent behaviour also
304 presents significant damage on the 3rd floor but only for four scenarios from the assessed 15.
305 When reducing the cross-section of the timber elements, it was observed that in-plane the
306 significant damage is also appearing on the second level of the building, according to the
307 FaMIVE limit state and that more scenarios are presenting significant damage according to the
308 combined prevalent behaviour.
309 The second roof structure develops a different type of distribution of the damage levels.
310 Therefore, the building is presenting significant in-plane damage mainly at the 2nd or combined
311 at the 2nd and 3rd floor according to the FaMIVE limit state. This roof structure is also causing
312 no damage considering the out-of-plane prevalent behaviour and significant damage on the 3rd
313 floor for the combined behaviour. The reduction of the cross-section of the timber element is
314 shifting the significant damage towards the 2nd floor of the building at the in-plane prevalent
315 behaviour according to the FaMIVE limit state and for the combined prevalent behaviour.
316 The 3rd roof structure is presenting significant damage only at the 3rd floor according to all limit
317 states for all three assessed prevalent behaviours (in-plane, out-of-plane and combined). The
318 reduction of the cross-section of the timber elements is completely changing the damage state
319 of the building. The structure would not suffer any in-plane damage according to EC8 but would
320 suffer additional significant damage at the 2nd floor according to the FaMIVE limit state. The

most peculiar observation is that the reduction of the cross-section of the elements is causing the complete disappearance of the damage for the out of plane prevalent behaviour.

Table 8 Damage state of the masonry building for relevant floors and numbers of scenarios where the damage state appears (D.l. – Damage limitation; S.d. – Significant damage; scen. – scenario)

			Roof 1		Roof 2		Roof 3	
		No roof	100%	-20%	100%	-20%	100%	-20%
In-plane								
CODES	**EC8 Part 3**							
	2nd floor	D.l.	D.l.	D.l.	D.l.	D.l.	D.l.	D.l.
	3rd floor	S.d.	-	-	-	-	S.d. *3scen.*	D.l.
	2nd + 3rd floor	-	-	-	-	-	-	-
CODES	**FaMIVE**							
	2nd floor	-	S.d. *1scen.*	S.d. *5scen.*	S.d. *7scen.*	S.d. *12scen.*	D.l.	-
	3rd floor	-	S.d. *9scen.*	S.d. *8scen.*	S.d. *1scen.*	-	S.d. *allscen.*	-
	2nd + 3rd floor	S.d.	-	S.d. *2scen.*	S.d. *5scen.*	S.d. *3scen.*	-	S.d. *allscen.*
	Experimental							
	2nd floor	D.l.	D.l.	D.l.	D.l.	D.l.	D.l.	D.l.
	3rd floor	S.d.	D.l.	S.d. *3scen.*	D.l.	D.l.	S.d. *allscen.*	S.d. *12scen.*
	2nd + 3rd floor	-	-	-	-	-	-	-
Out of plane								
CODES	**EC8 Part 3**	D.l.	D.l.	D.l.	D.l.	D.l.	D.l.	D.l.
	3rd floor	D.l.	D.l.	D.l.	D.l.	D.l.	D.l.	D.l.
CODES	**FaMIVE**	D.l.	D.l.	D.l.	D.l.	D.l.	D.l.	D.l.
	3rd floor	D.l.	D.l.	D.l.	D.l.	D.l.	D.l.	D.l.
	Experimental							
	3rd floor	S.d.	D.l.	D.l.	D.l.	D.l.	S.d. *5scen.*	D.l.
Combined								
	2nd floor	D.l.	D.l.	D.l.	D.l.	S.d. 12scen.	D.l.	D.l.
	3rd floor	S.d.	S.d. *4scen.*	S.d. *8scen.*	S.d. *3scen.*	D.l.	S.d. *allscen.*	S.d. *allscen.*

3.5. Internal forces

In in the last phase of the study the axial force, shear force and bending moment on the masonry walls were evaluated.

The axial force for the scenario without roof structure is presenting an apparent decrease with the elevation of the building. The presence of the roof structure is changing this completely. Therefore, while for the no roof structure scenario only compressive internal forces were

identified for all the floors of the building, the presence of the roof structure is introducing tension at the top of the building.

Evaluating the scenarios with complete cross-section of the timber elements it was observed that the first roof structure is causing tensile interior forces for all the scenarios at the top of the 2nd floor, the second at the bottom and the top of the 2nd floor while the third roof structure is keeping compressive interior forces at all the floors.

When reducing the cross-section of the timber elements, things change for all the assessed roof typologies (Figure 7). The first one is presenting slightly higher tensile interior forces at the top of the 2nd floor while the 2nd type is presenting tensile forces on the second floor, both up and down. The 3rd roof is also presenting tensile interior forces, but only for the semi-rigid joints, determined according to the equations of the component method and Heimeshoff.

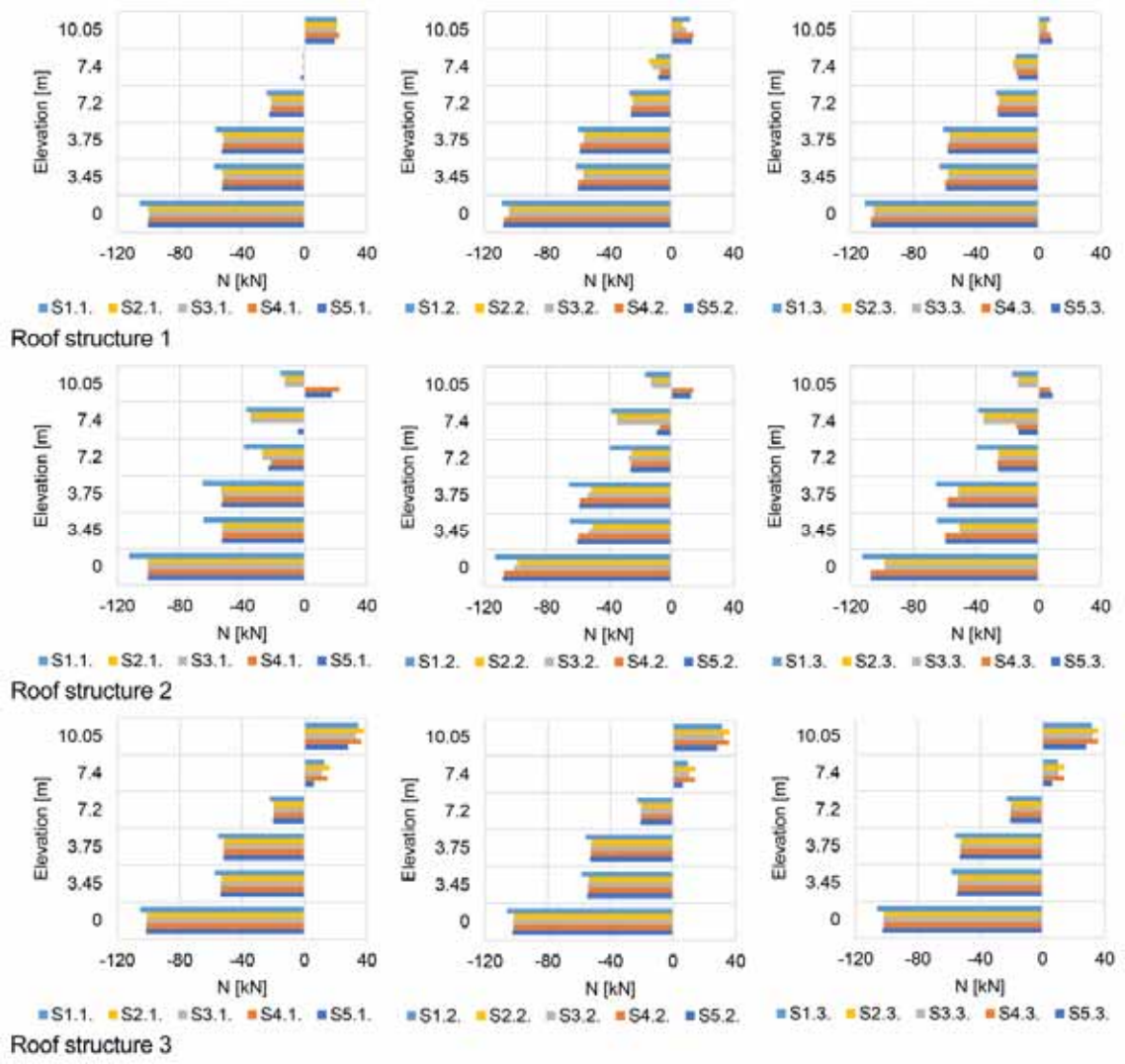

Figure 7 Axial forces recorded for the building with the three assessed roof structures (reduced cross section)

The shear forces and the bending moment are quite similar for all the three roof structures. For the complete cross-section of the timber elements it was observed that the first roof structure significantly influenced by the chosen joints and support scenarios. The highest internal forces were identified at the 2nd floor for rigid support scenarios and minimum internal forces at the top of the 1st floor while all the other scenarios are presenting a maximum at the top of the 1st floor decreasing towards the 2nd floor. The second and third roof structure present similar behaviours between the assessed scenarios. The second roof structure is presenting high

interior forces at the top of the 1st floor and minimum the 2nd floor, while the 3rd roof structure is presenting the maximum interior forces at the 2nd floor and minimum at the top of the 1st. When reducing the cross-section, no changes were observed (Figure 8).

A peculiar feature of the shear force is the presence of negative internal forces at the bottom of the 1st floor, due to the presence of the cross vault in that area. This behaviour was observed for all the roof types and all the assessed scenarios.

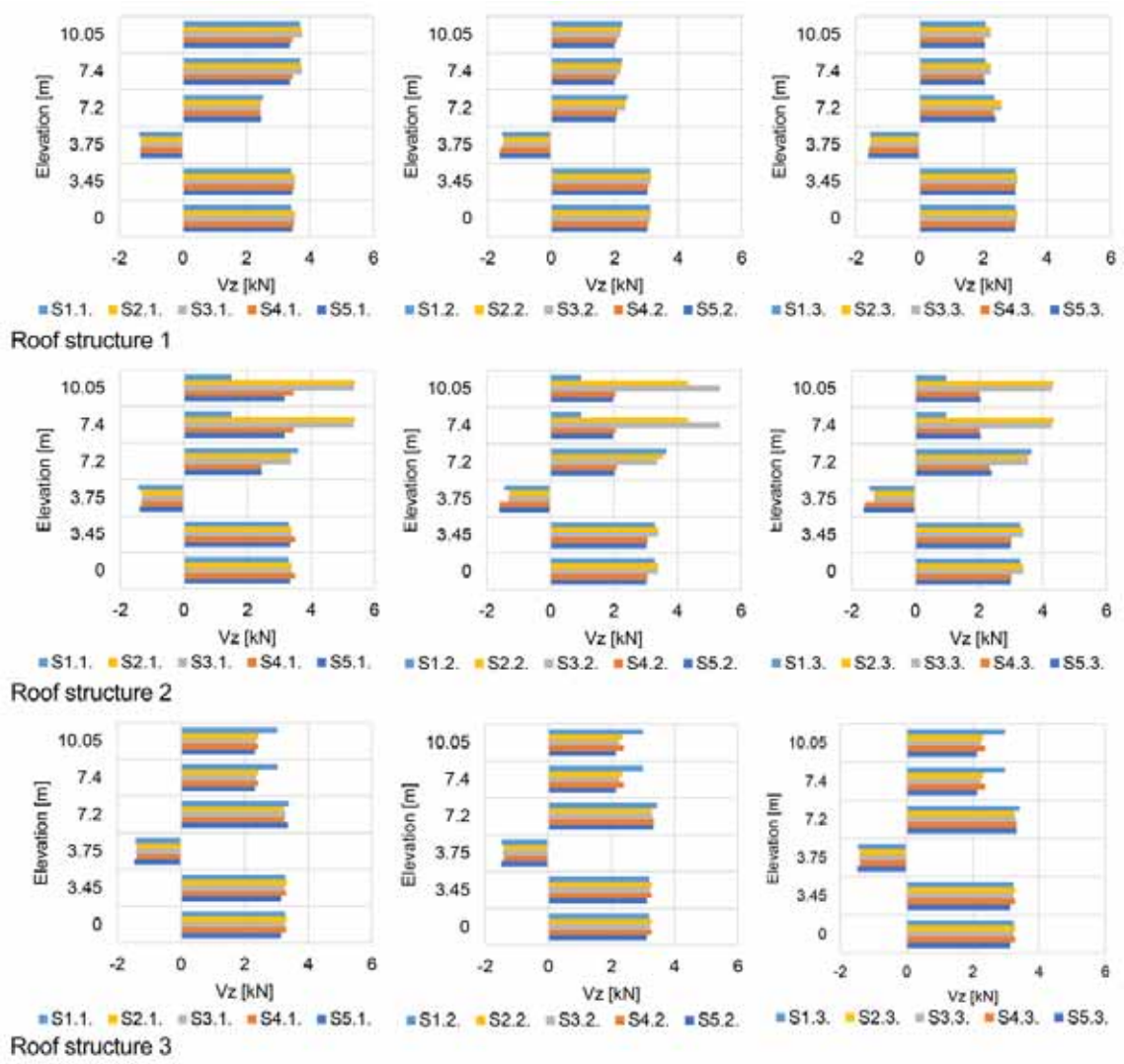

Figure 8 Shear forces recorded for the building with the three assessed roof structures (reduced cross section)

The bending moment analysis showed that all the roof structures are presenting a minimum bending moment at the bottom of the 2nd floor. Like in the case of the shear force no significant

differences were observed between the complete and the reduced cross section of the timber elements (Figure 9).

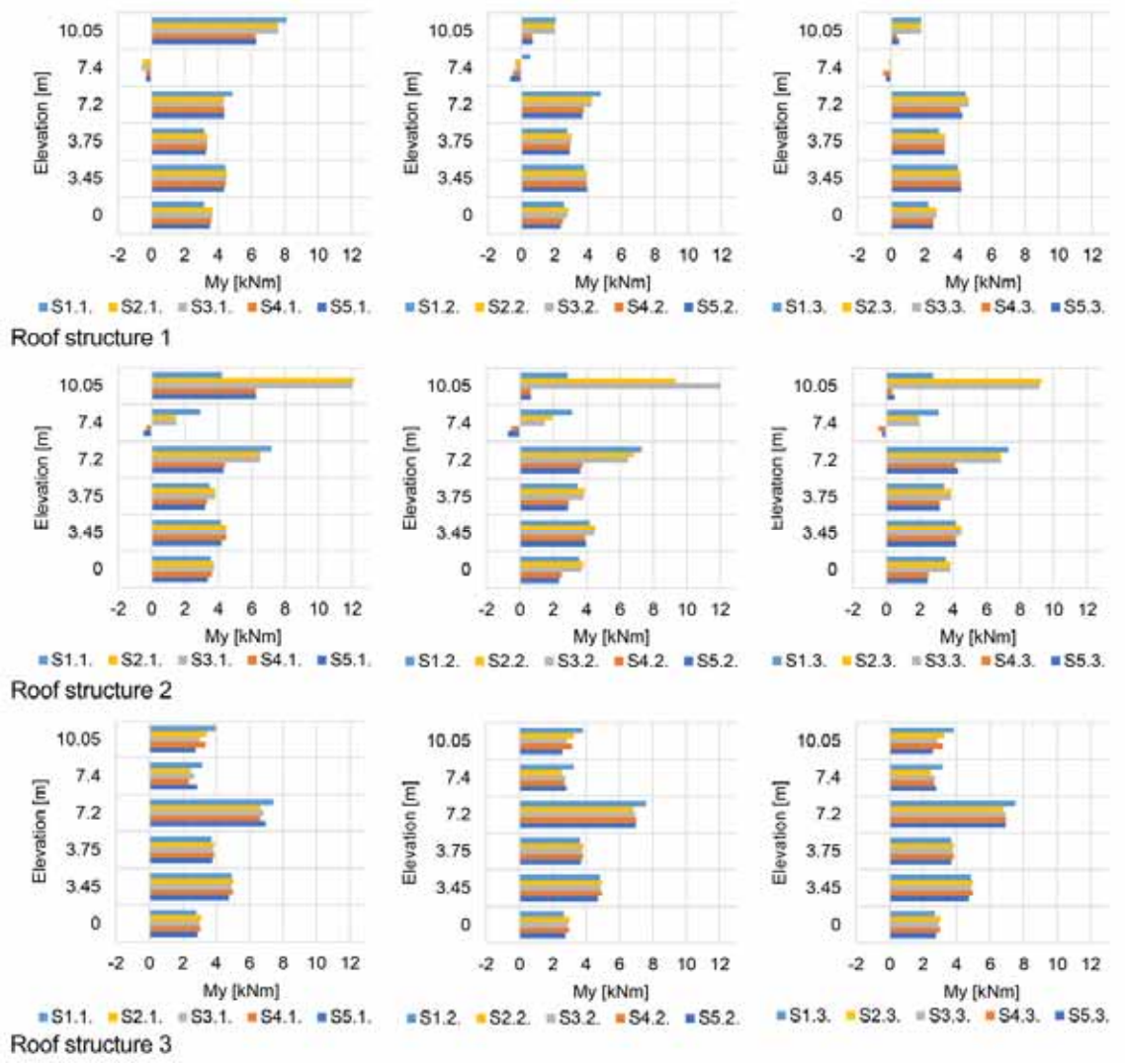

Figure 9 Bending moments recorded for the building with the three assessed roof structures (reduced cross section)

4. Conclusions

The study presents, by using numerical simulations, a first attempt to identify the influence of historic roof structures on the seismic behaviour of historic masonry buildings.

Due to their complex shape and interlinked elements, but also due to their connection to the masonry walls, historic roof structures from the 18th 19th and 20th century are significantly improving the seismic behaviour of masonry structures.

They are, according to the type:

- Reducing the top horizontal displacement between 20 and 40%;
- Reducing the inter-story drift from 25 up to 75%;
- Reducing the damage level of the masonry structure;
- Changing the deformed shape of the building from flexural to shear depending on the support and joint rigidity;

Besides, the study is highlighting

- the importance of the chosen joint stiffness, showing that hinged, rigid and semi-rigid joints can change the seismic response of the building
- that the decay of the timber elements is also changing the seismic behavior of the building:
    - increasing the displacement and inter-story drift for the 18th-century roof structure on all the floors;
    - decreasing them for the 19th and 20th-century structures on the 3rd floor while increasing them significantly on the 2nd floor.

Due to the complexity and diversity of historic roof structures, further studies are still necessary in order to identify how other structural typologies are influencing the seismic behaviour of heritage buildings, acknowledge their importance and be able to introduce new data into design codes.

List of notations

k_{ax} is the axial stiffness of timber joints

$E\alpha$ is the elastic modulus of the timber

α is the angle between the two timber elements composing the joint

S is the compressed surface of the joint

A is the compressed surface of the joint

A_{vert} is the contact surface which transfers the vertical load through the joint

A_{horiz} is the contact surface which transfers the horizontal load through the joint

b is the width of the timber element composing the joint

409 t_v is the depth of the notch of the joint

410 D.I. Damage limitation

411 S.d. Significant damage

412 scen. Scenario

413

414 **References**

415 Andreescu I, Keller A and Mosoarca M (2016) Complex Assessment of Roof Structures.
416 Procedia Engineering **161**:1204–1210. doi: https://doi.org/10.1016/j.proeng.2016.08.542.
417 Apostol I, Mosoarca M, Chieffo N and Onescu E (2019a) Seismic Vulnerability Scenarios for
418 Timisoara, Romania. In *Structural Analysis of Historical Constructions* (Aguilar, R., Torrealva,
419 D., Moreira, S., Pando, M. A. and Ramos, L. F. (eds.)). Springer International Publishing, Cham,
420 pp. 1191–1200.
421 Apostol I, Mosoarca M, Chieffo N and Onescu E (2019b) Seismic Vulnerability Scenarios for
422 Timisoara, Romania. In *Structural Analysis of Historical Constructions* (Aguilar R., Torrealva D.,
423 Moreira S., Pando M.A., R. L. F. (ed.)). Springer, Cham, vol 18., pp. 1191–1200.
424 Branco J and Descamps T (2015) Analysis and strengthening of carpentry joints. Construction
425 and Building Materials **97**:34–47. doi: https://doi.org/10.1016/J.CONBUILDMAT.2015.05.089.
426 Branco JM, Piazza M and Cruz PJS (2010) Structural analysis of two King-post timber trusses:
427 Non-destructive evaluation and load-carrying tests. Construction and Building Materials
428 **24**(**3**):371–383. doi: https://doi.org/10.1016/j.conbuildmat.2009.08.025.
429 Comite Europeen de Normalisation (2016) *BS EN 338:2016 Structural Timber. Strength*
430 *Classes*.
431 Cruz H, Yeomans D, Tsakanika E, Macchioni N, Jorissen A, Touza M, Mannucci M, Lourenço
432 PB (2015) Guidelines for On-Site Assessment of Historic Timber Structures. International
433 Journal of Architectural Heritage **9**(**3**):277–289. doi:
434 https://doi.org/10.1080/15583058.2013.774070.
435 D'Ayala D and Riggio M (2015) Assessment of Historical Timber Structures: Select Papers from
436 the Second International Conference on Structural Health Assessment of Timber Structures
437 (SHATIS13). International Journal of Architectural Heritage **9**(**6**):639–640. doi:

https://doi.org/10.1080/15583058.2015.1041356.

Descamps T and Lemlyn P (2009) Effects of the rotational, axial and transversal stiffness of the joints on the static response of old timber framings. In *Protection of Historical Buildings: Proceedings of the International Conference on Protection of Historical Buildings, PROHITECH 09* (Mazzolani, F. (ed.)). CRC Press, Rome, Italy, pp. 281–286.

Gaivoronschi V, Andreescu I and Mosoarca M (2013) Working in the Attic. Complex Restauration and Reconversion of an Historic Attic Structure in Timisoara, Romania. In *C60 International Conference Tradition and Innovation – 60 Years of Civil Engineering Higher Education in Transilvania*. Cluj, Romania, pp. 287–288.

Giresini L, Fragiacomo M and Sassu M (2016) Rocking analysis of masonry walls interacting with roofs. Engineering Structures **116**:107–120. doi: https://doi.org/10.1016/j.engstruct.2016.02.041.

Heimeshoff B and Kohler N (1989) *Assessment of the Structural Behaviour of Timber Joints (in German)*, Munchen.

Holzer SM (2015) *Statische Beurteilung Historischer Tragwerke. Band 2, Holzkonstruktionen*. Wilhelm Ernst & Sohn, a Wiley brand.

Holzer SM (2016) Analysis of historical timber structures. In *Structural Analysis of Historical Constructions – Anamnesis, Diagnosis, Therapy, Controls* (Van Balen & Verstrynge (ed.)). Taylor & Francis Group, Leuven, Belgium, pp. 1203–1210.

Keller A and Mosoarca M (2017) A complex assessment of historic roof structures. In *4th International Conference on Structural Health Assessment of Timber Structures (SHATIS'17)* (Arun, G. (ed.)). pp. 157–168.

Meisel A (2015) *Historische Dachwerke Beurteilung, Realitätsnahe Statische Analyse Und Instandsetzung*. Monographi. Verlag der Technischen Universität Graz, Graz.

Mosoarca M, Onescu I, Onescu E, Azap B, Chieffo N and Szitar-Sirbu M (2019) Seismic vulnerability assessment for the historical areas of the Timisoara city, Romania. Engineering Failure Analysis **101**:86–112. doi: https://doi.org/10.1016/J.ENGFAILANAL.2019.03.013.

Narita A, Mosoarca M, Modena C, da Porto F, Munari M, Taffarel S, Marson C., Valotto C., Roverato M (2016) Behavior of Historic Buildings in Zones with Moderate Seismic Activity. Case

467 Study: Banat Region, Romania. Procedia Engineering **161**:729–737. doi:
468 https://doi.org/10.1016/j.proeng.2016.08.754.
469 Nemetschek (2013) *SCIA Engineer User Manual*.
470 Parisi MA and Chesi C (2014) Seismic vulnerability of traditional buildings: the effect of roof-
471 masonry walls interaction. In *Tenth U.S. National Conference on Earthquake Engineering*
472 *Frontiers of Earthquake Engineering*. Anchorage, Alaska, (21-25/07).
473 Parisi MA, Chesi C and Tardini C (2012) The Role of Timber Roof Structures in the Seismic
474 Response of Traditional Buildings. In *15th World Conference on Earthquake Engineering*.
475 Lisbon, Portugal.
476 Parisi MA, Chesi C, Tardini C and Piazza M (2008) Seismic vulnerability and preservation of
477 timber roof structures. In *Structural Analysis of Historic Construction* (Dina, D. and Enrico, F.
478 (eds.)). Bath, United Kingdom, pp. 1253–1260.
479 Parisi MA, Tardini C and Maritato E (2016) Seismic behaviour and vulnerability of church roof
480 structures. In *Structural Analysis of Historical Constructions*. pp. 1582–1589.
481 Riggio M, D'Ayala D, Parisi MA and Tardini C (2018) Assessment of heritage timber structures:
482 Review of standards, guidelines and procedures. Journal of Cultural Heritage **31**:220–235. doi:
483 https://doi.org/10.1016/J.CULHER.2017.11.007.
484 Tonna S and Chesi C (2015) Wood reinforced masonry in poor construction traditions. In *3 Rd*
485 *International Conference on Structural Health Assessment of Timber Structures*. Wroclaw.
486 Touliatos P (2005) The box framed entity and function of the structures: the importance of
487 wood's role. In *Conservation of Historic Wooden Structures: Proceedings of the International*
488 *Conference*. Florence, Italy, (22-27/02), pp. 52–64.
489 Touliatos PG (1993) Traditional aseismic techniques in Greece. In *Proceedings of the*
490 *Interantional Workshop Les Sytèmes Nationaux Faces Aux Seismes Majeurs* (Mendés, V.
491 (ed.)). Lisbon, Portugal, pp. 110–124.
492 Vicente R, D'Ayala DF, Miguel TM, Varum H, Costa A, J M da S and Lagomarsino S (2014)
493 Seismic Vulnerability and Risk Assessment of Historic Masonry Buildings. In *Structural*
494 *Rehabilitation of Old Buildings*. pp. 307–348.
495 Wallner B, Ortner J, Gregor S, Bogensperger T, Meisel A, Augustin M and Schickhofer G (2014)

imber-Timber Joints (in German)*. Graz.

(2013) *Romanian Seismic Design Code P 100-1/2013*.